Naval Research Laboratory
Stennis Space Center, MS 39529-5004

NRL/FR/7174--95-9629

Modeled High-Frequency Acoustic Backscattered Levels from Range-Independent and Simplistic Range-Dependent Sand Bottoms

KRISTEN D. SAVAGE

Planning Systems, Inc.
Slidell, LA 70458

ROGER W. MEREDITH

Ocean Acoustics Branch
Acoustics Division

February 21, 1996

Approved for public release; distribution unlimited.

REPORT DOCUMENTATION PAGE

Form Approved
OBM No. 0704-0188

1. AGENCY USE ONLY *(Leave blank)*

2. REPORT DATE
February 21, 1996

3. REPORT TYPE AND DATES COVERED
Final

4. TITLE AND SUBTITLE
Modeled High-Frequency Acoustic Backscattered Levels from Range-Independent and Simplistic Range-Dependent Sand Bottoms

5. FUNDING NUMBERS
Job Order No. 571686006
Program Element No. 0602435N
Project No. RO35E420EO
Task No.
Accession No. DN153130

6. AUTHOR(S)
Kristen D. Savage* and Roger W. Meredith

7. PERFORMING ORGANIZATION NAME(S) AND ADDRESS(ES)
Naval Research Laboratory
Acoustics Division
Stennis Space Center, MS 39529-5004

8. PERFORMING ORGANIZATION REPORT NUMBER
NRL/FR/7174--95-9629

9. SPONSORING/MONITORING AGENCY NAME(S) AND ADDRESS(ES)
Naval Research Laboratory
Marine Geosciences Division
Stennis Space Center, MS 39529-5004

10. SPONSORING/MONITORING AGENCY REPORT NUMBER

11. SUPPLEMENTARY NOTES
*Planning Systems, Inc., 115 Christian Lane, Slidell, LA 70458

12a. DISTRIBUTION/AVAILABILITY STATEMENT
Approved for public release; distribution unlimited.

12b. DISTRIBUTION CODE

13. ABSTRACT *(Maximum 200 words)*

Results investigating the effects of variable bottom composition on modeled high-frequency backscattered levels are presented for a typical shallow-water, variable bottom (range-dependent) environment. The modeled environment consisted of a single sound speed profile, a flat sea bottom with range-dependent bottom composition, and a smooth, flat sea surface. Coarse- and fine-grained sandy areas were partitioned in range to create range dependence. Bottom backscattering and reflection loss for each partition were obtained from the recent University of Texas high-frequency ocean bottom backscatter model (N. P. Chotiros and F. A. Boyle, J. Acoust. Soc. Am., vol. 96, no. 5, pt. 2, 3264, (1994)). Maximum differences of 5 dB were discernible between the fine-coarse-fine sand bottom and a range-independent fine-sand bottom for ranges <500 m. The trend and structure of the backscattered levels were nearly identical for both bottom types. In all cases, surface reverberation had a strong impact on the backscattered levels, trends, and structures.

14. SUBJECT TERMS
sonar source depth, range-dependent bottom, range-independent bottom, sand, mine countermeasures

15. NUMBER OF PAGES
16

16. PRICE CODE

17. SECURITY CLASSIFICATION OF REPORT	18. SECURITY CLASSIFICATION OF THIS PAGE	19. SECURITY CLASSIFICATION OF ABSTRACT	20. LIMITATION OF ABSTRACT
Unclassified	Unclassified	Unclassified	Same as report

NSN 7540-01-280-5500

Standard Form 298 (Rev. 2-89)
Prescribed by ANSI Std. Z39-18
298-102

CONTENTS

MODELED HIGH-FREQUENCY ACOUSTIC BACKSCATTERED LEVELS FROM RANGE-INDEPENDENT AND SIMPLISTIC RANGE-DEPENDENT SAND BOTTOMS

1.0 INTRODUCTION

Detecting all objects of mine-like size from a safe standoff distance is the objective of minehunting. Regardless of whether the objects are floating within the water column, proud on the seafloor, or partially buried within the seafloor, detection occurs when the sonar discriminates between the object and its background environment. Discrimination is optimized by maximizing the difference between the echo produced by a target when compared to the background (i.e., sonar contrast). The background typically consists of ambient noise, surface, volume, and bottom reverberation. This model study presents the effects of variability in bottom composition on the mean background reverberation level for a generic minehunting sonar in shallow water.

Sonar performance models assist mine countermeasure (MCM) commanders in assessing sonar system performance and adjusting sonar parameters, as well as in mission planning and post-mission analysis. For ship and personnel safety, it is imperative that performance estimates are accurate (or at worst, conservative). Regardless of the type of sonar—sector scan, side scan, or synthetic aperture—they are characterized by small angular beamwidths (<3°) and fine-range resolution (<1.5 m). High acoustic frequencies (>20 kHz) and short ping lengths (<5 ms) are employed to achieve these characteristics. These sonar signals are processed and analyzed over ranges typically less than 1500 m.

The optimal operation of the sonar requires matching the sonar system to the acoustic environment to maximize target return signal and minimize background noise and reverberation. Approaches to maximizing detection probability typically depend on the interfering background. If noise controls the detection range, then both the frequency and bandwidth of the sonar ping can be adjusted. Alternatively, if reverberation is the predominant background, then the source level, beamwidth, and pulse length of sonar ping may be adjusted. In shallow water, the seafloor and sea surface raise reverberation levels, present false targets to the sonar system signal processor, and degrade coherence of acoustic energy scattered from the boundaries.

In support of research, operational forces, and sonar design, a wide variety of sonar performance models have been developed and tested [1–8]. The Range Dependent Active System Performance Prediction Model (RASP) [9] was used in this study to compute mean reverberation level by incoherent averaging of individual ray intensities. Bottom backscattering and reflection loss values used in RASP were obtained from the recent Applied Physics Laboratory/University of Texas (APL/UT) high-frequency ocean bottom backscattering model [10] based on Biot's theory. Bottom variability was introduced by quadrupling grain size.

In this study, the modeled environment consists of a single sound speed profile, a flat sea bottom (30-m depth), and a smooth, flat sea surface. Mean reverberation is modeled for two separate

source/receiver geometries and for both range-independent and range-dependent bottom compositions. Although the sonar performance model employed for this study may be too computer intensive to provide near-real-time results during an actual MCM mission, it may be valuable in mission planning and training. Portions of this report were included at the 129th meeting of the Acoustical Society of America.

2.0 RASP ACOUSTIC MODEL

The RASP model [9] was designed for deep-water, long-range propagation at frequencies below 1 kHz and its roots trace back to the 1960s at Hudson Laboratories [11]. The model was selected for this study in part because of local access to expert users. It is currently being used in data fusion studies of acoustic and magnetic measurement data to predict acoustic transmission loss [12,13], and is also currently used in sonar design and performance prediction [14] and was used to develop the Bottom Distributed Active Simulation System [15] under the Air Defense Initiative. It is one of the few ray trace models with environmental range-dependent capabilities. There are other sonar performance models with similar forms of environmental range-dependence capabilities, PC_RAYTRACE [7] and MOCCASIN [8]. These and several other sonar performance models are readily available and have recently been summarized [16–19].

In general, RASP fits each sound speed profile to a cubic spline function that is then used in numeric ray tracing. Acoustic intensities along the path are estimated from a numerical solution to the basic wave equation incrementally obtained point to point along each path. Boundary reverberation is estimated from ray intensities along paths that join the source and receiver to each insonified area of the boundary. Travel time and grazing angles are also calculated. The total time-dependent reverberation is determined by integrating contributions from each insonified area. Mean reverberation level as a function of time can be calculated with or without a target present. RASP traces one ray at a time and defines ray families based on the number of path reversals.

2.1 Modeled Environment

The environment inputs are based on measurements at a site approximately 100 miles south of Panama City, FL, during the month of August, 1993. The Naval Research Laboratory conducted experiments on high-frequency (20–200 kHz) bottom scattering [20]. The thermodynamic properties of the ocean medium determine acoustic sound speed and how acoustic energy will propagate in the water column. The sound speed often varies with depth and the resulting sound speed gradients cause the acoustic ray to refract or bend in the direction of decreasing sound speed. The input sound speed profile for this study was an average of six daytime sound speed profiles spanning the 1-week experiment. It consisted of a single profile containing 28 depth/sound speed pairs. The bottom composition was a mixture of fine- and coarse-grain sands. The input to the bottom scattering strength model (discussed in subsequent sections) was based on grain sizes and surface roughness observed at the experimental site. No attempt was made to model sand ridges.

2.2 PROFIL Module

The module PROFIL assembles the range-dependent environment based on bottom bathymetry and multiple sound speed profiles containing sequential depth/sound speed pairs. Since our interest was a short-range, shallow-water environment, a flat bottom with a constant depth of 30 m was used.

2.3 RAYACT Module

RAYACT determines the ranges and associated ray statistics of ray–path encounters with the surface and bottom boundaries. RAYACT applies an iterative procedure incrementing point to point along each ray path by Taylor series expansions of arc lengths. RAYACT also computes travel time and ray angle. The maximum number of boundary interactions plus ray reversals was set to the default value of 198. Three fans of ray launch angles were used to estimate reverberation. The upper fan contains 24 launch angles (from −89° to 5°) and the lower fan consists of 19 launch angles from 15° to 89°. The middle fan uses 50 launch angles from 5° to 15° to emulate a downward-looking sonar. The upper and lower fans significantly improve the linear interpolation of the range–angle contours for intensity calculations [14]. Figure 1 displays the 28-point sound speed profile and the resulting ray trace for a source/receiver depth of 3 m. Modeled results span ranges 0–2 km in .01-km increments.

2.4 RTHETA Module

The module RTHETA converts the results from RAYACT into range-order contours based on the number of ray reversals as well as determines the presence of caustics. If specified, the wave-theoretic correction is applied. All available angles are processed with no discrete source angles nulled. RTHETA weights the rays by beam patterns and computes ray amplitudes and phases. The Francois-Garrison formula [21] for volume acoustic attenuation was used based on the integrated sound speed. The attenuation value, 5.3 dB/km, was input into RASP. RASP calculates attenuation based on horizontal range rather than actual ray path. This is acceptable at this frequency as long as the water column is segmented into enough layers. RTHEATA assumes single plane scattering, thus RASP may yield higher reverberation levels than may be measured due to losses resulting from out-of-plane scattering.

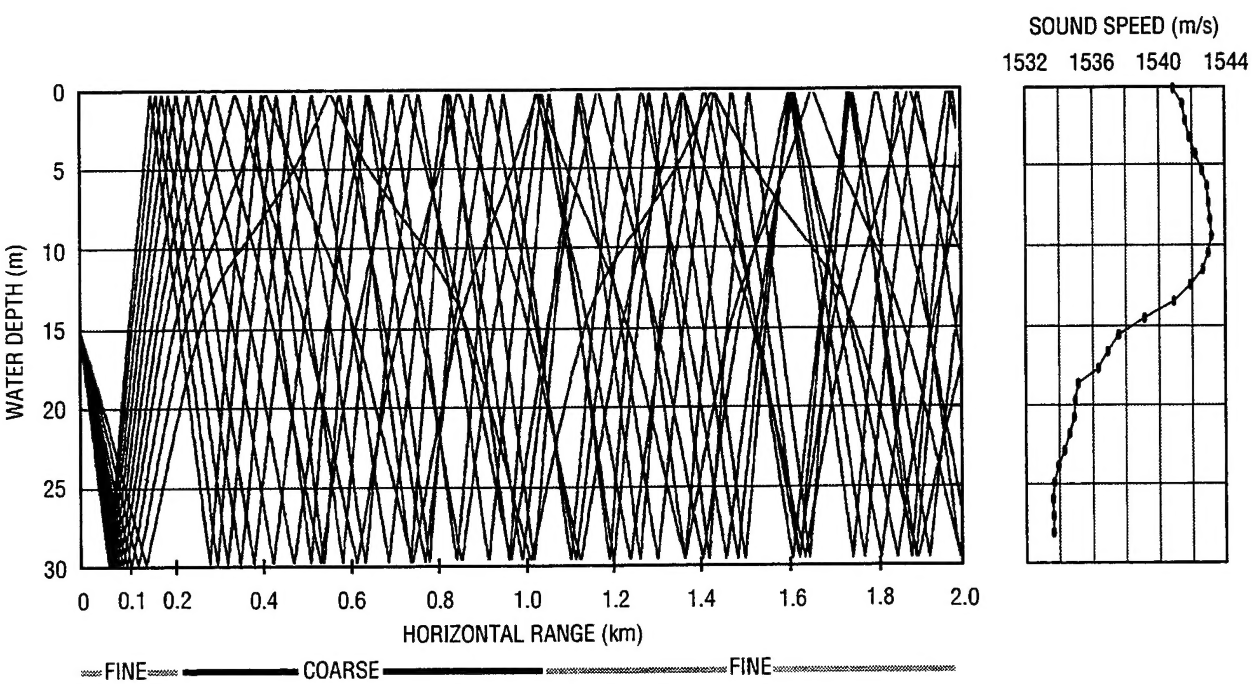

Fig. 1 — Typical RASP ray trace for 3-m source/receiver depth and the sound speed profile used for this study. The range-dependent bottom partitions are illustrated and only a few of the beams representing the main sonar beam are shown.

2.5 TLVSR Module

The module TLVSR computes the transmission loss as a function of range by interpolating the ray arrival order contours to determine ray intensities. For this work, incoherent transmission loss was used and, thus, a mean reverberation envelope is returned. Experience has shown that the computed shallow-water short-range transmission loss may be lower than that computed from a parabolic equation (PE) model.

2.6 REVERB Module

The module REVERB calculates the total reverberation levels and target echo levels as a function of time or launch angle. No targets were modeled in this study. RASP does not propagate acoustic energy through the bottom, but can account for energy loss into the bottom via the bottom loss vs. grazing angle table that may be input. This was done using bottom loss tables for both fine- and coarse-grain sand obtained from the recently published ARL/UT model developed by Chotiros and Boyle [10, 22].

2.7 ACTENV Module

Using a target object parameter, acoustic source parameters, and results from REVERB, ACTENV computes a mean received level. Since no target objects were used in this study, the mean received level is the mean reverberation level. The source frequency was 35 kHz with a 10-ms ping length. The ambient noise level was set to –128 dB, well below the mean reverberation level for the ranges examined. The output mean reverberation level is provided as a surface reverberation component and a bottom reverberation component.

2.8 Surface Scattering Model

This study concentrated on bottom variability effects on reverberation. The surface scattering component was modeled to be as benign and perfectly reflecting as possible. RASP defaults to the surface scattering model of Chapman-Harris [23]. Sea-state zero was always used. This surface model has some known deficiencies, especially at low grazing angles for low wind speeds where surface scattering is underestimated.

2.9 Bottom Scattering Model

Bottom scattering is a critical component of MCM sonar performance modeling because most mine-like objects are located in, on, or near the seafloor. Acoustic scattering is complex due to surface roughness, composition, and sediment layering. Bottom backscattering is complicated by several factors including acoustic frequency, grazing angle, bottom density, and roughness, as well as by sound speed, bottom absorption, porosity, and layer thickness. Recently, a new high-frequency ocean bottom backscattering model was introduced by Chotiros and Boyle and the Applied Research Laboratory of the University of Texas at Austin [10].

The new model is based on three physical mechanisms: scattering from sediment grains, scattering from interface roughness, and scattering from entrained gas bubbles. At lower grazing angles, sediment grains and gas bubble scattering dominate; at higher grazing angles, interface roughness dominates. The acoustic reflection loss and penetration into ocean sediments is based on Biot's theory. The bubble backscatter component is based on resonant scattering from gas bubbles trapped in the sediment. The grain scattering component is based on empirical fits to experimental data. The

interface roughness component is based on numerical integration of the Kirchoff-Helmholtz scattering integral.

For this study, the gas bubble fraction was set to zero so that no component of scattering was due to resonant scattering from gas bubbles. The interface roughness was kept constant. The input differences in the two bottom types are grain size and the coarse-grain size is four times the size of the fine-grain size (2.25 mm diameter and 9 mm diameter, respectively). This yields differences in sediment porosity and in the absorption coefficients used in the Biot model.

Figure 2 shows plots of backscatter strength and the forward loss vs. grazing angle for both the coarse- and fine-grain sand generated by the ARL/UT model and used in the RASP model environment. At lower grazing angles, the changes in reverberation levels will be due more to backscattering strength since the forward scattering loss is nearly constant. At middle to high grazing angles, the forward scattering loss causes differences in reverberation level since there is little change in backscattering strength.

3.0 RASP PRELIMINARY TESTING

3.1 Ray Trace Tests

Since RASP was designed for long-range, deep-water propagation, a test of the ray tracing capability was in order for short-range, shallow-water application. The Sonar Performance Model (SPM) [24]

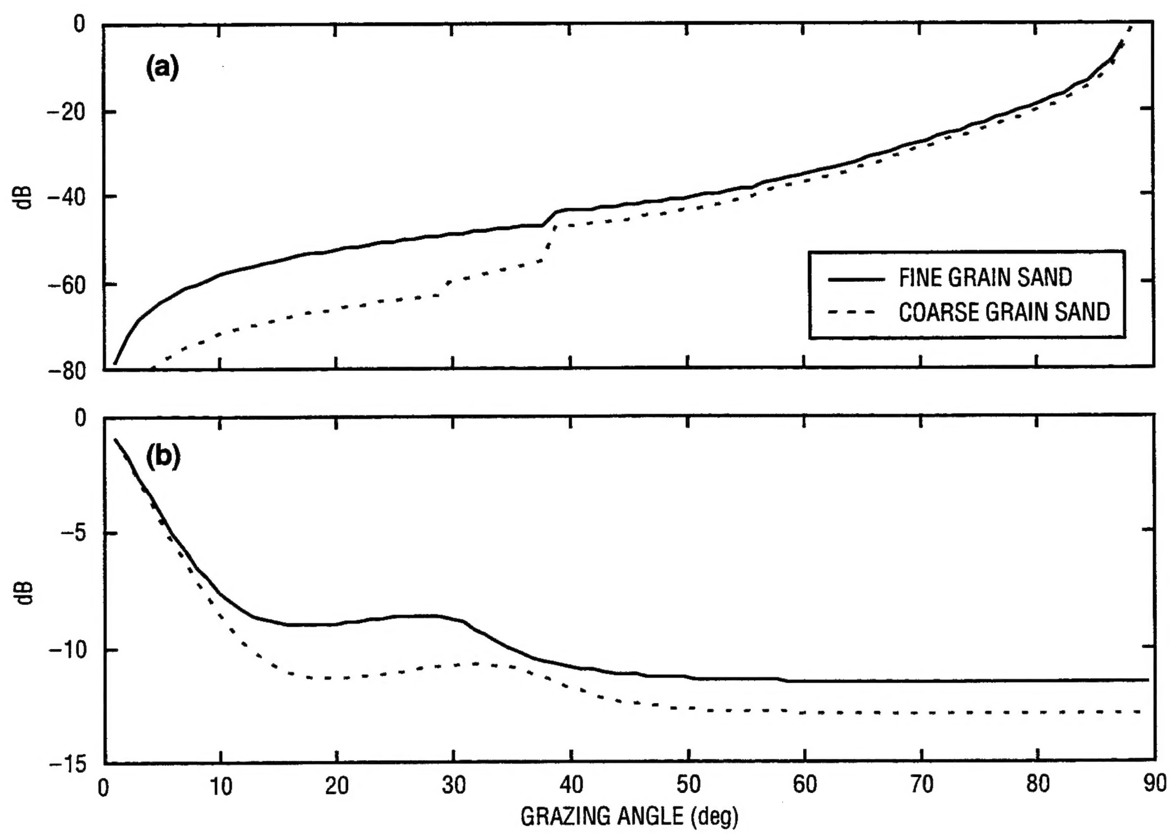

Fig. 2 — Results from ARL/UT High Frequency Bottom Backscatter Model: (a) backscattering strength and (b) forward scattering loss used as environmental input into RASP

was chosen as a baseline for comparison with RASP ray trace. SPM is a recent derivative of SEARAY [2, 25] currently in use by U.S. Naval MCM forces. Two different sound velocity profiles were chosen for comparison. The first test used the sound speed obtained from the continental shelf near Panama City, FL. This sound speed is the same one used in subsequent modeling of reverberation levels. No differences in the ray traces between SPM and RASP were observed. The second test used a hyperbolic cosine function for sound speed. Many general purpose ray tracing algorithms use a horizontally stratified water column where the sound velocity is a piece-wise linear function of depth. Such cases provide complex ray trajectories composed of lines, circles, hyperbolas, and other shapes within each stratum [26]. To accurately ray trace a cosh sound speed, a large number of strata are required, thus providing a good test of ray tracing algorithms. No differences were observed between SEARAY and RASP ray traces in either test, the shallow-water or short-range. No differences between RASP ray trace and Fig. 2.1 of Ref. 26 were observed in a long-range, deep-water test.

3.2 Transmission Loss Test

As a second test of RASP's use in shallow water, a comparison of one-way transmission loss (TL) with the finite element parabolic equation (FEPE) model is shown in Fig. 3. TL is plotted as a function of range for incoherent and coherent ray intensity averaging within RASP along TL from FEPE. Since FEPE does not include a volume attenuation term, attenuation was set to zero within

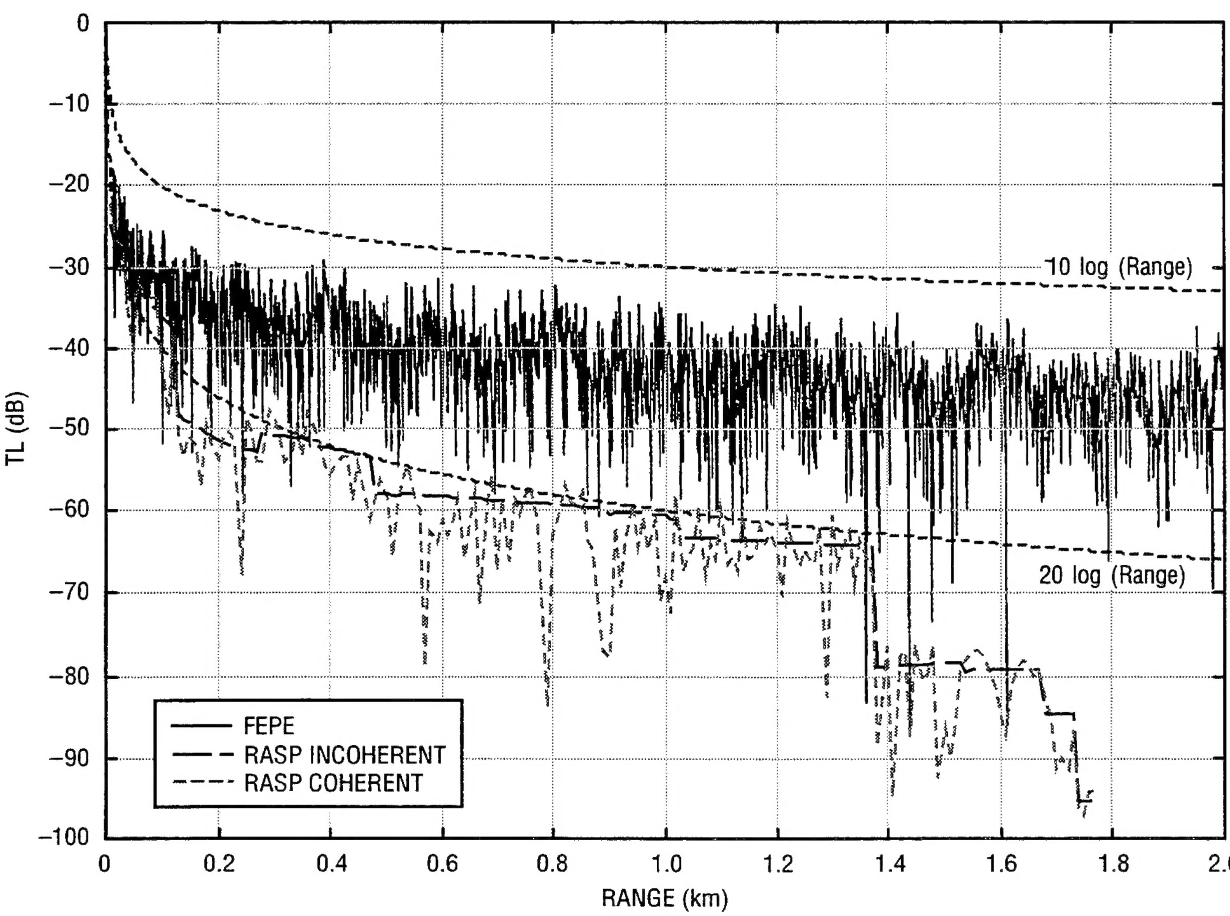

Fig. 3 — Comparison of one-way transmission loss from RASP and from FEPE

RASP. RASP modeled TL for evenly spaced rays from –90° to 90° relative to the horizontal. FEPE employed an order of magnitude smaller range step in computations than did RASP. The bottom parameters used in FEPE were density (2.65 g/cm^3), sound speed (1807 m/s), and attenuation (1.43 dB/wavelength).

For horizontal ranges out to 0.2 km, which includes first bottom bounce, TL matches well, both in levels and scalloping locations. From 0.2–1.4 km the scalloping is similar (spanning 20 dB), but locations in range are different and the TL levels are very different. The best smooth fit through FEPE is similar to incoherent average but 20 dB higher in level. Each major step in the RASP TL corresponds to a new set of multipath arrivals. For this test, TL is composed only of spreading and bottom loss effects. How much of the difference in TL is from bottom loss and how much is from spreading loss is not known at this time. Other researchers have found good agreement between RASP and FEPE TL results for lower frequencies and deeper water scenarios [14]. These differences may be due to invalid comparison, but clearly require closer examination. The purpose here is not to compare FEPE and RASP, but to examine the effect of range-dependent bottom types on reverberation level.

3.3 RASP Sample Ray Trace

Figure 1 is a ray trace from RASP displaying water depth vs. range. For clarity, only the rays from the main sonar beam are shown. The maximum water depth is 30 m with a source depth at 15 m. This scenario results in grazing angles of approximately 15–30°. Therefore, from Fig. 2, effects due to changes in both the backscatter strength and the forward scattering loss of the two bottom types contribute to changes in the reverberation level. The first bottom bounce occurs at 55 m and the surface interaction is at 150 m. The range-independent case consists of all fine-grain sand, and for the range-dependent case, the bottom is composed of fine-grain sand from 0–200 m, followed by a partition of coarse-grain sand spanning 200–1000 m. A third partition of fine-grain sand spans the range of 1000–2000 m. The single sound speed used in this study was measured at a site on the continental shelf off Panama City, FL. The grain sizes are loosely based on the grain sizes observed at the same site.

4.0 COMPARISON OF RASP ESTIMATIONS

4.1 Purpose, Method, and Implementation

The goal of this modeling study is to ascertain and quantify the effects of variable range-dependent bottom composition on the mean reverberation level received by a typical high-frequency minehunting sonar in a typical shallow-water minehunting scenario. The mean reverberation level, in decibels, is computed as a function of time (range) by the RASP model by incoherent averaging of ray intensities. In this report, differences in mean reverberation envelope level are compared for different scenarios.

- *Range-Independent Bottom* – Range-independent bottom means that the bottom composition is not a function of range and that only one bottom type is used in the model. One range-independent bottom is used in this study, composed only of fine-grain sand.
- *Range-Dependent Bottom* – A range-dependent bottom implies that the bottom composition changes as a function of range. One range-dependent bottom is used in this study consisting of three components: fine-grain sand from 0–200 m, coarse-grain sand from 200–1000 m, followed by fine-grain sand from 1000 m.
- A near-surface sonar source depth (3-m depth).

• A near-bottom sonar source depth (15-m depth or 13 m above the bottom).

Four descriptors are used to facilitate comparison of mean reverberation levels:

• the mean reverberation level as a function of range (time) as predicted by the model;

• the overall trend in level, i.e., best straight line fit to the reverberation envelope;

• the structure and pattern of reverberation level over smaller range scales (interrelation of the reverberation levels in a complicated entity);

• the transition range is defined as the range at which reverberation from the surface interaction intersects and dominates the reverberation from the bottom interaction.

Unless otherwise noted, mean reverberation level refers to only the bottom component of reverberation in which the bottom was the last boundary interaction prior to reaching the receiver.

4.2 Shallow Source Depth: Range-Independent and Range-Dependent Bottom Types

This section compares the differences in the range-independent reverberation from the fine-grain sand bottom with range-dependent reverberation from the fine-coarse, fine-grain sand bottom for a source/receiver depth of 3 m. Figure 4 shows a plot of the RASP surface and bottom components

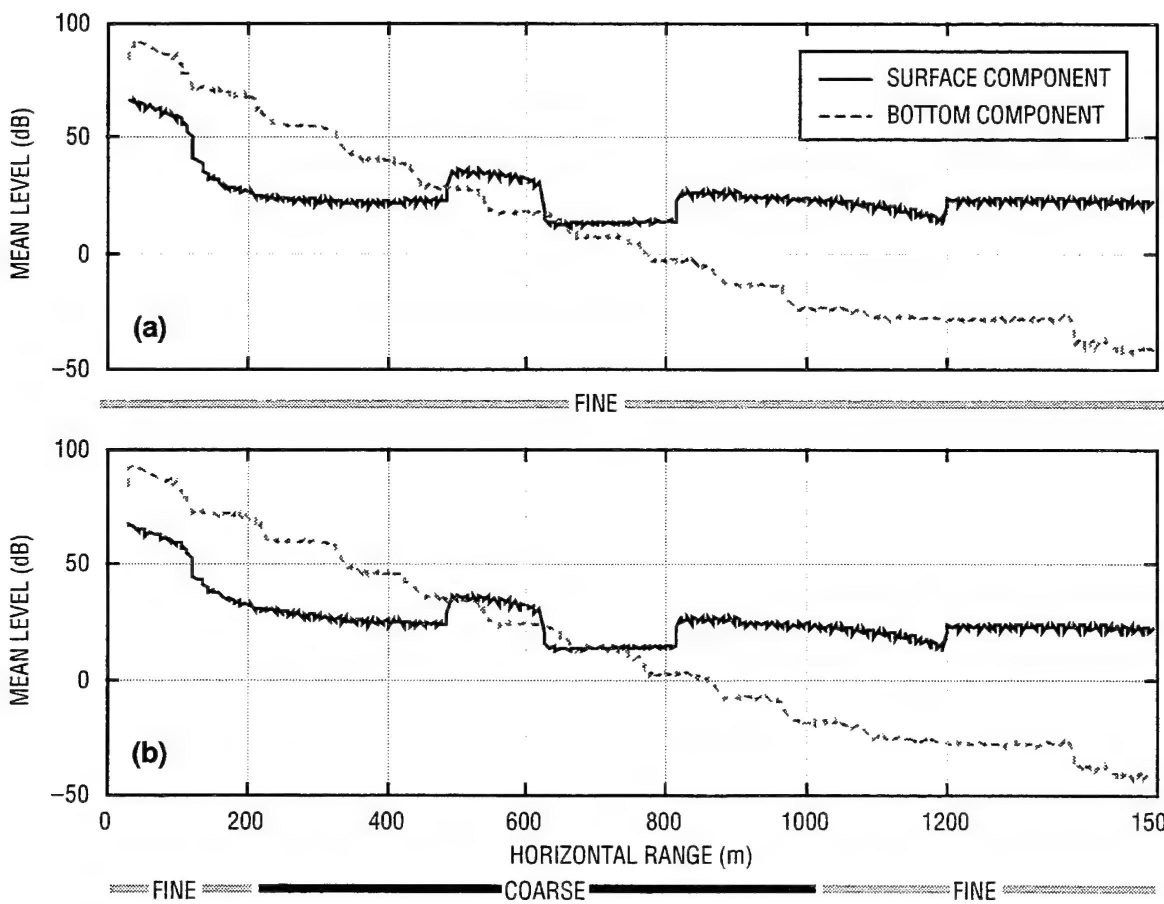

Fig. 4 — RASP modeled reverberation levels as a function of range for 3-m source/receiver depth in both (a) range-independent and (b) range-dependent bottoms. The range-dependent bottom partitions are illustrated and the mean reverberation level is partitioned into surface and bottom components.

of mean reverberation levels. The surface components are identical and only the bottom components are discussed. The upper plot is the range-independent fine-grain sand bottom and the lower plot is the range-dependent fine-coarse, fine-grain sand bottom. For ranges less than 220 m, the bottom types are the same and the bottom components of mean reverberation levels are identical. This range encompasses the first bottom bounce, the first surface bounce, and the second bottom bounce. The stair-step structure of the bottom reverberation is similar for both bottom types and is due to multipath interference. From 220 m out to the transition range of 480 m, the overall range-dependent bottom (lower plot) yields a 5 dB higher level than the range-independent bottom (upper plot). Beyond 480 m, the reverberation is surface dominated. Between 480 m and 1.2 km, the mean reverberation level remains 5 dB higher for the range-dependent bottom (lower plot). For ranges less than 1.2 km, both the trend and structure are similar.

4.3 Deep Source Depth: Range-Independent and Range-Dependent Bottom Types

This section compares the differences in the range-independent reverberation and range-dependent reverberation for a source/receiver depth of 15 m. Figure 5 shows a plot of mean reverberation levels broken up into surface and bottom components. Again, the surface components are identical and only the bottom components are discussed. The upper plot is the range-independent fine-grain sand bottom and the lower plot is the range-dependent fine-coarse, fine-grain sand bottom. Similarly, for ranges less than the second bottom bounce near 220 m, the mean reverberation levels are nearly

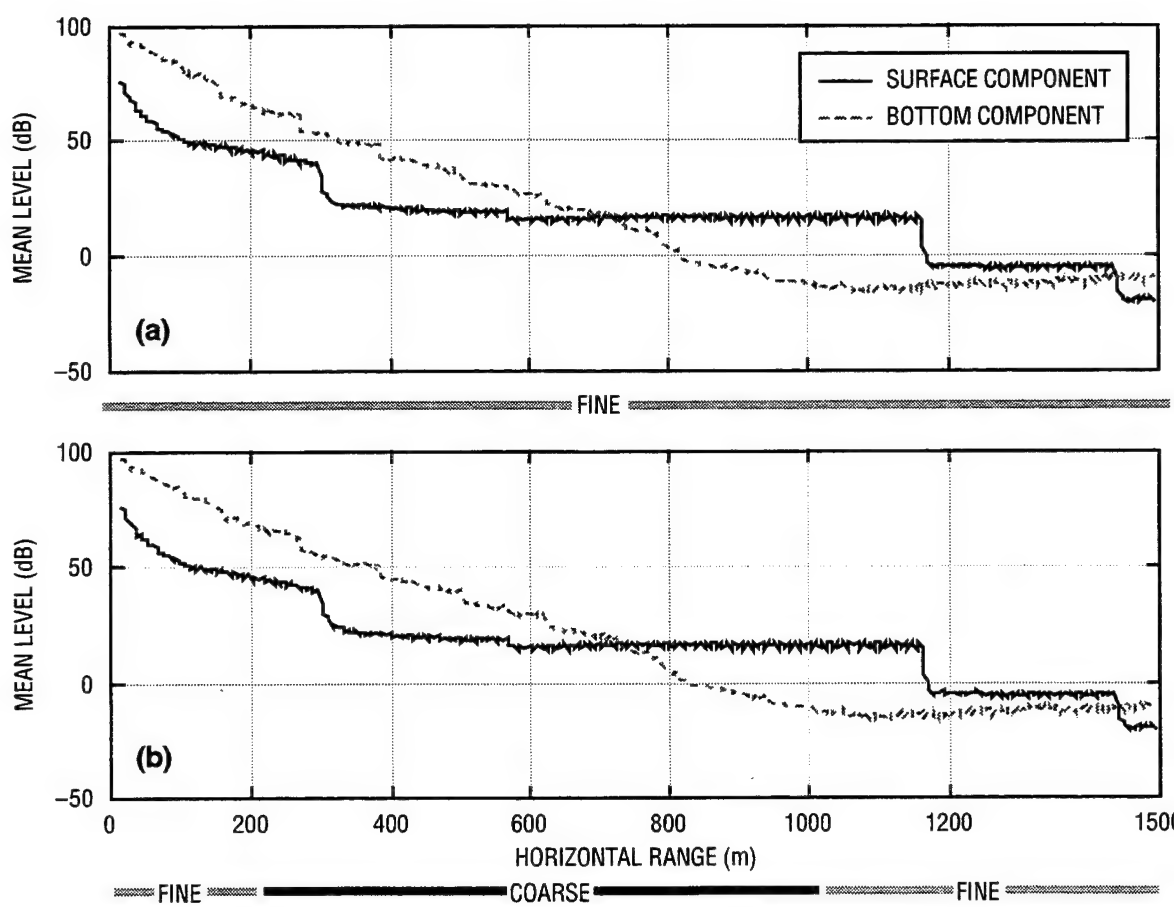

Fig. 5 — RASP modeled reverberation levels as a function of range for 15-m source/receiver depth in (a) range-independent and (b) range-dependent bottoms

identical. The stair-step structure of the bottom reverberation is due to multipath interference and is reduced approximately 2 dB from Fig. 4. The mean reverberation level from the range-dependent bottom (lower plot) is 3 dB higher than from the range-independent bottom (upper plot) for ranges spanning 220 m to the transition range of 700 m. For ranges spanning 700 m to 1.2 km, the range-dependent bottom remains 3 dB greater in received level. The trend and structure of the received level as a function of range are nearly identical for all ranges.

4.4 Range-Independent Bottom Type: Deep Source Depth and Shallow Source Depth

This section compares the differences in Figs. 4 and 5. One difference is the range at which the dominant reverberation changes from the bottom to the surface. Figures 4 and 5 show that for a 3-m source/receiver depth, the transition range occurs near 480 m, while for a source/receiver depth of 15 m, the transition range is 700 m. This is due to geometry and not to bottom type. Figure 6 shows the differences in the bottom component of mean reverberation level. The range-independent level minus the range-dependent level is plotted vs. horizontal range for both the 3- and 15-m source/receiver depths. For ranges between 220 and 1000 m, the difference in mean reverberation levels due to bottom variability is less than 3 dB for the deeper 15-m source/receiver depth, and

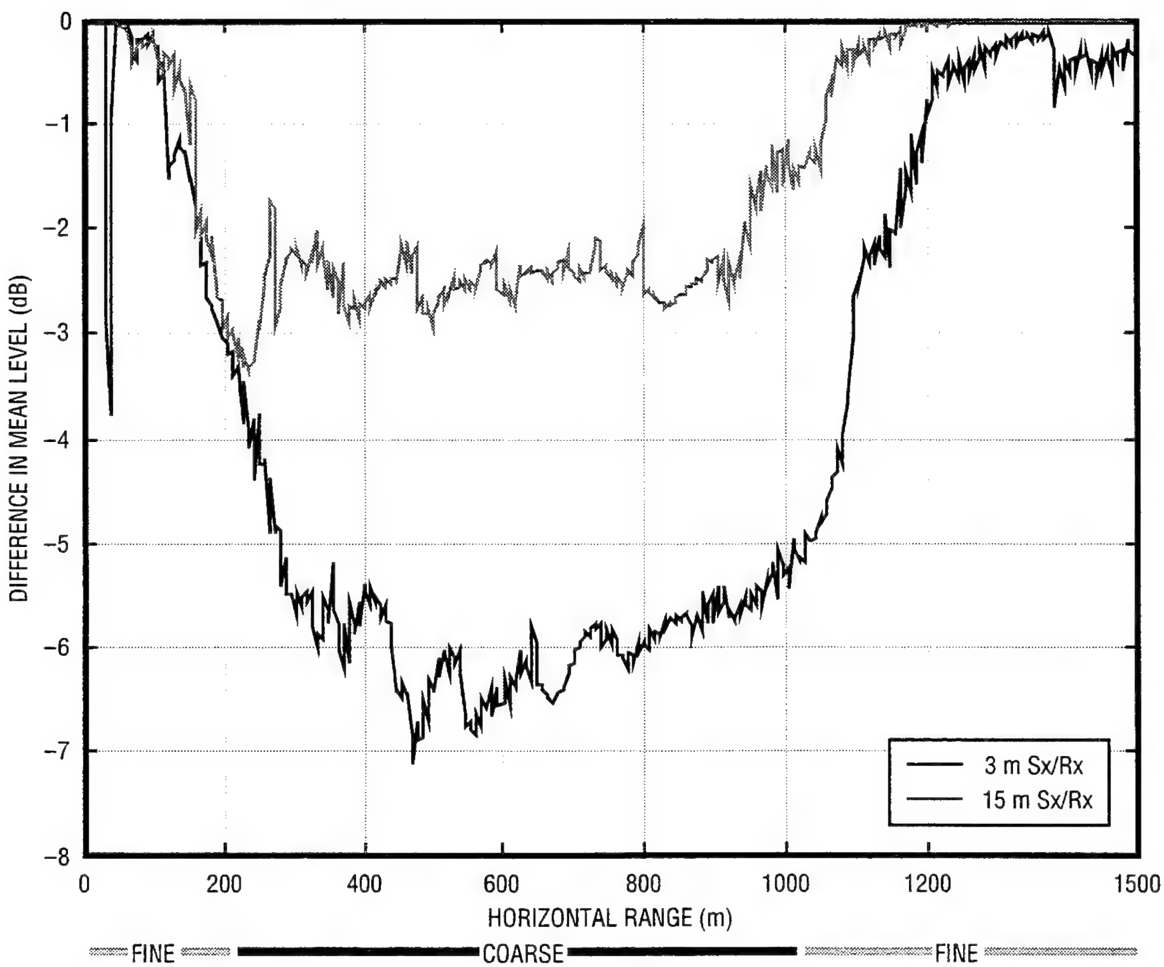

Fig. 6 — Difference in bottom reverberation components of mean reverberation levels predicted by RASP. The difference, range-independent minus range dependent, is plotted for both source/receiver depths separately.

the difference is greater than 5 dB for the 3-m source/receiver depth. Thus, the shallower source/receiver is more sensitive to bottom variability than the deeper source/receiver by as much as 3 dB. The deeper source exhibits a smoother, flatter difference as a function of range, but in neither case is the fluctuation more than 2 dB. For ranges out to 1.2 km, the mean reverberation level for the deeper source depth averages 3–5 dB greater than the shallower source depth.

4.5 Range-Dependent Bottom Type: Deep Source Depth and Shallow Source Depth

This section compares the differences between the 3-m source/receiver depth (Fig. 4) and the 15-m source/receiver depth (Fig. 5) for both the range-independent and range-dependent bottom compositions. Figure 7 shows the differences in the bottom component of mean reverberation level. The 3-m source/receiver level minus the 15-m source/receiver level is plotted vs. horizontal range for each bottom composition. For ranges between 220 and 1000 m, the differences for the range-dependent bottom are shifted upward by 3 dB in mean reverberation level. However, the peak-to-peak differences and fluctuations in the differences are nearly identical for both the range-independent and range-dependent bottom types. The structure and trend of the differences in bottom components of reverberation level are similar.

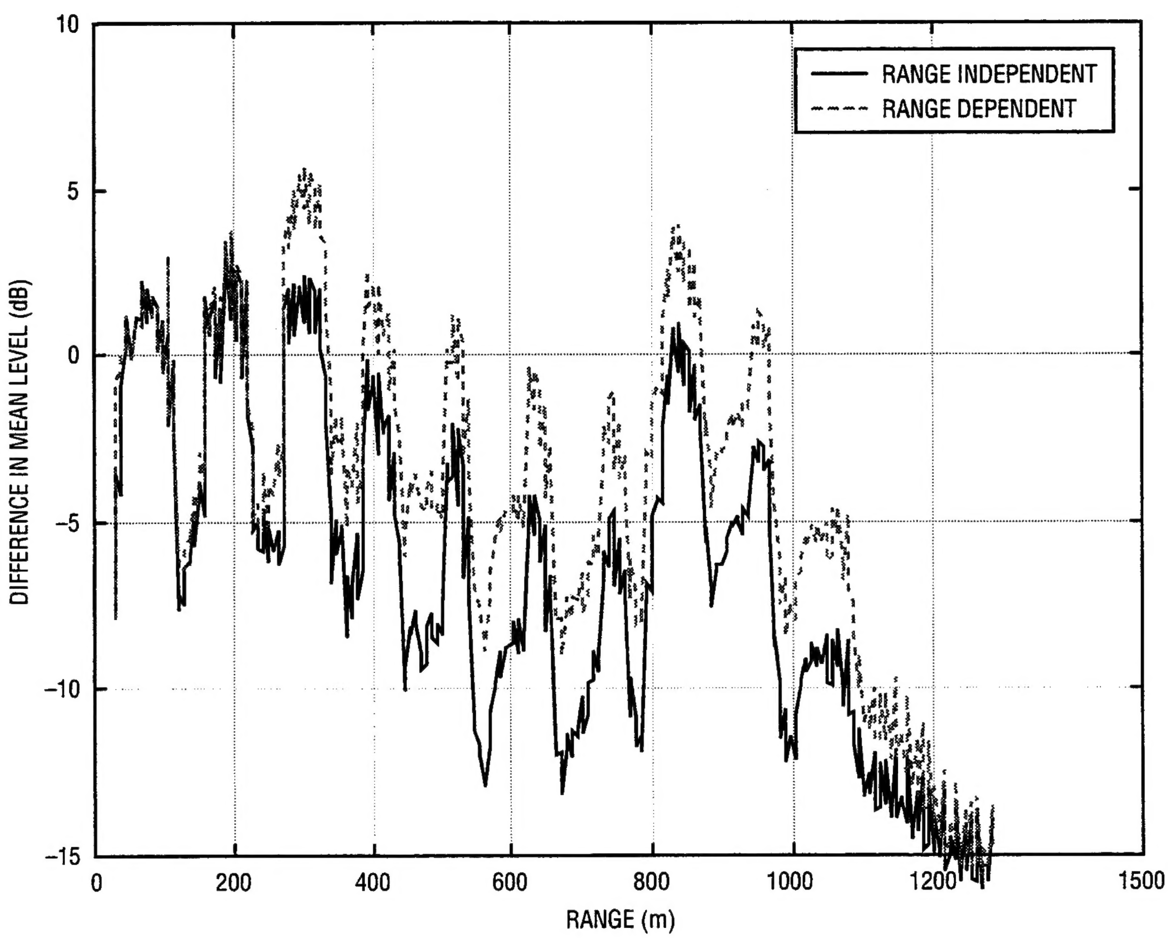

Fig. 7 — Difference in bottom reverberation components of mean reverberation levels predicted by RASP. The difference, 3-m source/receiver depth minus 15-m source/receiver depth, is plotted for both range-independent and range-dependent bottom types separately.

5.0 SUMMARY AND CONCLUSIONS

The goal of this modeling effort was to ascertain and quantify the effects of simple range-dependent bottom composition on the mean reverberation level received by a typical high-frequency minehunting sonar in a typical shallow-water scenario. Differences in mean reverberation level were compared for different scenarios:

- range-independent bottom consisting of fine-grain sand;
- range-dependent bottom consisting of three partitions of fine- and coarse-grain sand;
- a near-surface sonar source depth (3-m depth); and
- a near-bottom sonar source depth (15-m depth or 13 m above the bottom).

Comparison of mean reverberation levels included overall trends in level, the structure and pattern of reverberation level over smaller range scales, and the range at which reverberation from the surface dominates the reverberation from the bottom interaction.

The model results indicate that simplistic range-dependent bottom environments can affect shallow-water reverberation levels created by typical minehunting sonars and that this effect is stronger for shallower source/receiver geometries. The simplistic range-dependent bottom used here employed a coarse-grain sand partition flanked by fine-grain sand. The coarse-grain sand increased the mean reverberation level by approximately 2 dB for the 15-m source/receiver and 6 dB for the 3-m source/receiver. The coarse-grain sand partition had little or no effect on the trend and structure of the reverberation levels and no effect on the location of the transition range from bottom-dominant to surface-dominant reverberation. Simple changes in bottom composition led to changes in reverberation levels that may account for target fading and less accurate predictions of sonar detection ranges.

This was one example of range-dependent bottom types on reverberation. Other examples with different sizes and numbers of partitions quickly come to mind that bear testing. The surface scattering plays and important role in shallow water even at short ranges. More research is needed to accurately model surface reverberation and develop a range dependence.

6.0 ACKNOWLEDGMENTS

The authors are deeply grateful to Teenia Perry and Melvin Wagstaff for sharing their expertise with RASP, and also to David Bell. We acknowledge Nick Chotiros and Frank Boyle for access and guidance with their high-frequency bottom scattering model. This work was supported by the MCM Tactical Environmental Data System (MTEDS) under Program Element 0602435N, Sam Tooma, program manager.

7.0 REFERENCES

1. C. E. Jaster and H. Boehme, "The MINERAY Sonar Performance Prediction Computer Model Baseline Description," Technical Report No. 84-9 (ARL-TR-84-9), Applied Research Laboratories, University of Texas at Austin, Austin, TX, 1984.

2. S. M. Tuovila and L. E. Bowen, "SEARAY: A Modification of the MINERAY Sonar Performance Prediction Computer Model," NCSC Letter Report 3220-U-83-02, Naval Coastal Systems Center, Panama City, FL, 1983.

3. L. E. Bowen, "Preliminary Documentation Report Overviewing the Capabilities of CASTAR," NCSC Letter Report 3220-U-83-023, Naval Coastal Systems Center, Panama City, FL, 1983.

4. H. Weinberg, "Generic Sonar Model," NUSC Technical Document 5971D, Naval Underwater Weapons Center, Newport, RI, 1985.

5. J. R. Ventura, "High Frequency Environmental Acoustic Model (HFEAM)," NUWC-NPT Technical Document 10,114, Naval Underwater Weapons Center, Newport, RI, 1992.

6. H. Weinberg, "Effective Range Derivative for Acoustic Propagation Loss in a Horizontally Stratified Ocean," *J. Acoust. Soc. Am.* **70**(6) (1981).

7. B. Damsgaard, "User's Guide to PC-RAYTRACE, an Underwater Acoustic Detection Model," Report DDRE M-18/1991, Forsvarets Forskningstjeneste, 1991.

8. H. G. Schneider, "Mocassin—Sound Propagation and Sonar Range Prediction Model for Shallow Water Environments," TR-1990-9, Forschungsanstalt der Bundeswehr fur Wasserschall-und Geophysik, Germany, 1990.

9. L. B. Palmer and D. M. Fromm, "The Range-Dependent Active System Performance Prediction Model," NRL Formal Report 9383, Naval Research Laboratory, Washington, D.C., 1992.

10. N. P. Chotiros and F. A. Boyle, "A New High Frequency Ocean Bottom Backscattering Model," *J. Acoust. Soc. Am.* **96**(5), Pt. 2 (1994).

11. E. R. Franchi, J. M. Griffin, and B. J. King, "NRL Reverberation Model: A Computer Program for the Prediction and Analysis of Medium- to Long-Range Boundary Reverberation," NRL Formal Report 8721, Naval Research Laboratory, Stennis Space Center, MS, 1982.

12. T. T. Perry and W. M. Sanders, "The Application of the Bayesian Fusion Detection Criterion to the Case of Two Disparate Signals," 127th Meeting of the Acoustical Society of America, Cambridge, MA, 6–10 June, 1994.

13. J. K. Fulford, "Shallow Water RASP Upgrade," NOARL Technical Note 135, Naval Research Laboratory, Stennis Space Center, MS, 1991.

14. M. Wagstaff, Planning Systems Incorporated, Slidell, LA, private communication.

15. M. Bradley, M. Wagstaff, and B. Bradley, "Software Requirements for the Bottom Distributed Active Simulation System (BASS) Model Version 1.1," PSI-TRS204, AEAS TE-92-105, Planning Systems Incorporated, Slidell, LA, 1992.

16. R. Thiele, "A Comparative Test of Shallow-Water Sound Propagation Models Against Real Data," SACLANTCEN Special Report SR-149, LaSpezia, Italy, 1989.

17. R. W. Meredith and D. J. Ramsdale, "Survey and Overview of MCM Sonar Performance Models," The Technical Cooperation Program (TTCP), Subgroup G – Undersea Warfare Symposium, Heriot-Watt University, Edinburg, Scotland, 11–15 July, 1994.

18. R. W. Meredith and N. P. Chotiros, "Environmental Acoustic Modeling for MTEDS," NRL Memo Report 7534, Naval Research Laboratory, Stennis Space Center, MS, 1995.

19. L. B. Dozier and R. C. Cavanagh, "Overview of Selected Underwater Acoustic Propagation Models," AEAS Report 93-101, McLean, VA, 1993.

20. S. E. Stannic, E. Kennedy, and R. Goodman, "High Frequency Acoustic Bottom Reverberation," 128th Meeting of the Acoustical Society of America, 28 Nov–2 Dec., 1993.

21. R. E. Francois and G. R. Garrison, "Sound Absorption Based on Ocean Measurements: Part I: Pure Water and Magnesium Sulfate Contributions," *J. Acoustic. Soc. Am.* **72**(3), 896–907 (1982).

22. H. Boehme and N. P. Chotiros, "Acoustic Backscattering at Low Grazing Angles from the Ocean Bottom," *J. Acoust. Soc. Am.* **84**(3), 1018–1029 (1988).

23. R. P. Chapman and J. H. Harris, "Surface Backscattering Strengths Measured with Explosive Sound Sources," *J. Acoust. Soc. Am.* **34**(10), 1592–1597 (1962).

24. "Software User's Manual for the Sonar Performance Model Version 1.0," Coastal Systems Station Code 2110, Dahlgren Division, Naval Surface Warfare Center, Panama City, FL, 1992.

25. G. B. Dowling and G. S. Slasman, "CASTAR/SEARAY Environmental Reference Manual," Analysis and Technology, Inc., 124 Gwyn Dr., Panama City, FL, 1992.

26. R. W. McGirr, D. B. King, J. A. Davis, and J. Campbell, "An Evaluation of Range-Dependent Ray Theory Models," NORDA Report 115, Naval Research Laboratory, Stennis Space Center, MS, 1985.